

Cavity optimization of optically pumped broad-area microcavity lasers

S. Barbay,^{a)} Y. Ménesguen, I. Sagnes, and R. Kuszelewicz
*Laboratoire de Photonique et de Nanostructures, LPN/CNRS-UPR20, Route de Nozay,
91460 Marcoussis, France*

(Received 15 September 2004; accepted 3 March 2005; published online 8 April 2005)

We demonstrate a cavity optimization method for efficient optical pumping of a semiconductor microcavity. An enhanced pumping efficiency makes it possible to pump broad-area microcavities for, e.g., high-power lasers or parallel optical processing of information. This is especially important in the near-infrared where a pump not absorbed into the active material is absorbed into the substrate and converted into heat. We apply the method to optical pumping of a 80 μm diameter laser with a spatially uniform pump profile. This method could also prove useful for the design of vertical external cavity surface emitting lasers. © 2005 American Institute of Physics.

[DOI: 10.1063/1.1905781]

Broad-area microcavities are promising systems for applications to high power vertical cavity surface emitting lasers (VCSELs)^{1,2} or to parallel optical information processing with cavity solitons.³ These systems need high pump power to reach the laser threshold and are sensitive to the spatial gain profile.⁴ For such applications, optical pumping represents an advantageous technique compared to electrical injection. Indeed, with the advent of high-power fiber-coupled semiconductor sources, it is now possible to combine the shaping of the pump beam profile with the availability of high enough pump power. However, there are several issues associated with optical pumping of microcavities. The most important is how to efficiently couple the pump light into the cavity. A related question is how to reduce the temperature increase due to the pump absorption, since a large part of the energy that does not contribute to the material gain is converted into heat. A temperature increase of the device has several major effects: a shift of the cavity resonance towards larger wavelengths and a reduction of the material gain for a given carrier population, hence, requiring more pump energy and producing more heat. To obtain a higher quantum efficiency of the pump, it is necessary that the pump photon energy be close to the laser photon energy, since the carriers created at higher energies cascade to the bottom of the bands emitting phonons. Pumping in the sidebands of the Bragg mirrors has already been demonstrated and has become a common technique to reduce this energy loss. However, as noted by Knopp *et al.*,⁵ this technique remains difficult because of the cavity spectrum shift with temperature induced by the pump. Very efficient pump absorption can also be obtained by pumping resonantly in a narrow resonance close to the cavity stop band, but then bistability in the pump beam prevents a smooth operation.⁶ This also requires a pump laser with a small linewidth and adjustable wavelength, that precludes the use of high-power semiconductor laser arrays and, hence, limits the available pump power and pumped diameter.

Several approaches have been proposed to avoid these problems: opening a large pumping window in the reflectivity spectrum of the cavity with thin-film optimization techniques⁵ loosens the requirements on the spectral charac-

teristics of the pump source. To prevent further heating, post-processing the device in order to reduce heat production and/or enhance heat evacuation has also been used.^{7,8} Provided that the major source of heat for AlGaAs-based near-infrared devices comes from the pump absorption in the sample substrate, transparent (glass or AlGaAs) substrates may be employed. However, these techniques are not entirely satisfactory: glass is a very poor heat conductor and AlGaAs substrates do not allow for a good crystallographic quality of the samples.

We therefore propose to use Bragg mirror layer optimization techniques to, at the same time, increase the pumping efficiency and reduce the heat absorption by the substrate. These techniques are well known for the design of dielectric stacks with given specific properties but are far less used with semiconductors, although semiconductor growth is now well mastered for standard materials. The idea is to find a layer stack that matches a chosen target reflectivity, transmittivity, and absorption spectrum. This inverse problem is theoretically very challenging but can be solved numerically with optimization algorithms. Given the physical requirements stated earlier, we seek a stack with a low transmittivity and reflectivity of the entire layer structure over a broad spectral range around the pumping wavelength while maintaining a high finesse around the laser wavelength. This in turn implies a high absorption of the pump and an insensitivity of the pumping efficiency to thermal drifts of the cavity spectrum. Indeed, since the cavity transmission is proportional to the backmirror reflectivity, this implies a high reflectivity of the backmirror at the pump wavelength, preventing substrate heating by the pump and allowing a multiple pass of the pump into the active medium for higher pump absorption. At difference with Ref. 5, the pumping efficiency and the transmission at the pump wavelength are explicitly included in the optimization procedure. Moreover, pumping at an angle or with a high numerical aperture source becomes possible (as is the case with fiber-coupled high-power diode laser arrays) since the overall cavity response will be in that case integrated over the blueshifted angular dependence of the cavity response. This is of first importance when dealing with broad area devices for which usual pump sources, such as Ti:sapphire lasers, do not deliver enough power to reach the laser threshold. The method used is not restricted to mi-

^{a)}Electronic mail: sylvain.babay@lpn.cnrs.fr

croavity lasers and may also be of interest to the design of external cavity semiconductor lasers.

To test these ideas, we design a structure composed of $\text{Al}_{0.22}\text{Ga}_{0.78}\text{As}/\text{AlAs}$ multilayer mirrors, a λ_0 optical length GaAs layer as active material surrounded by two $\text{Al}_{0.07}\text{Ga}_{0.93}\text{As}$ absorbing spacers of variable length and a GaAs substrate. The role of the absorbing spacers (while being transparent to the laser wavelength) is to increase the pump light absorption. The carriers photogenerated in the absorbing spacers are then transferred to the GaAs active layer, thus contributing to a threshold reduction and increasing the pump absorption. The width of the pumping window is determined by considering the spectral characteristics (wavelength, spectral width) of the pump source, the expected operating temperature and the numerical aperture of the focusing optics onto the sample. We aim at a 30 nm width pumping window, in which the cavity transmittivity T_t and reflectivity R_t will be zero (or equivalently absorption A_t equals 1). At the lasing wavelength of 890 nm, the target reflectivity and transmittivity of the cavity should also be zero. The actual stack that matches these requirements is obtained with an optimization procedure. We build an error function $\xi[\mathbf{l}=(l_1, l_2, \dots, l_n)]$ of the layer thicknesses l_i that measures the deviation of a given stack characteristics (reflectivity R , transmittivity T , absorption A) with the ideal one we seek

$$\xi(\mathbf{l}) = \sum_i a_i [R(\lambda_i) - R_t(\lambda_i)]^2 + b_i [T(\lambda_i) - T_t(\lambda_i)]^2 + c_i [A(\lambda_i) - A_t(\lambda_i)]^2,$$

where the sum runs over all the target wavelengths λ_i . The a_i, b_i , and c_i are weight coefficients such that absorption is considered in the pumping window while reflectance and transmittance are considered at the cavity resonance. In general, with aperiodic (nonquarter-wave) multilayer mirrors the field maximum inside the cavity at resonance may neither coincide with the center of the cavity, nor with the pump field maximum. This would become a major issue in the case of a multiquantum well active material and shall be addressed in a future work. However, in the present case, carrier diffusion spreads the initial excitation along the thin active medium length. This releases the constraints on pump and laser field alignment inside the cavity. The optimization algorithm (we use a simple SIMPLEX algorithm⁹) stops when a local minimum of the function ξ is found with an acceptable balance between accuracy and computation time. The result (Fig. 1) is a completely irregular stack of layers with different widths. The total length of the structure is 8687 nm. The calculated reflectance spectrum (Fig. 2) shows a large window in the pump wavelength range around 800 nm, while at the same time the transmission is kept below 10% and absorption is around 75%. It should be stressed that this result is obtained without the inconvenience of resonant pumping as in Refs. 6 and 10. The cavity resonance around 890 nm anticipates a small temperature increase in the active medium close to threshold due to the residual pump transmission into the substrate. Even larger absorption are theoretically possible with larger absorbing spacers, but we wished not to excessively increase the overall length of the cavity for good longitudinal mode selection and ease of growth. A proper analysis of the spacer length optimum would require to take into account the carrier dynamics in

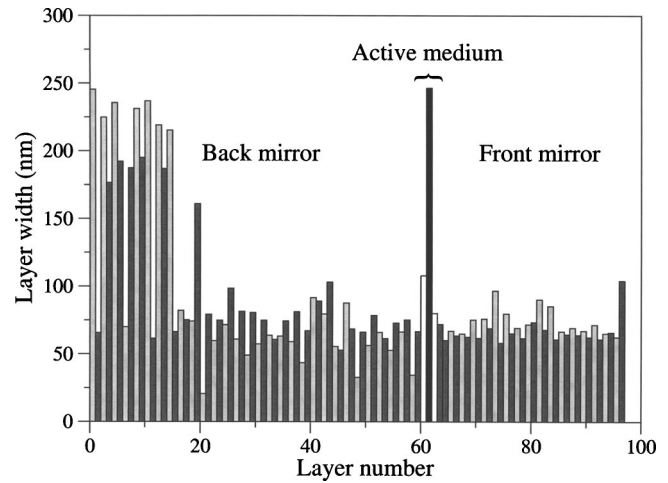


FIG. 1. Layer widths of the optimized structure. The substrate is on the left of the figure. The cavity is filled by two absorbing $\text{Al}_{0.07}\text{Ga}_{0.93}\text{As}$ spacers (layers 61 and 63, white bars) around a bulk GaAs active layer (layer 62, in black). The back and front Bragg mirrors are composed of alternating $\text{Al}_{0.22}\text{Ga}_{0.78}\text{As}$ (dark gray) and AlAs (light gray) layers.

the active and the spacer layers, as too long spacers imply a very long transit time of the carriers to the active layer compared to the characteristic stimulated recombination time.

The earlier designed layer stack has been grown by metalorganic chemical vapor deposition. The experimental reflectance spectrum is in very good agreement with calculations (Fig. 2). The shape of the absorption is measured by illuminating a small area of the sample with a Ti:sapphire laser with intracavity etalons. Doing so, one can make sure that the incidence of the pump beam onto the cavity is quasi normal. We then measure the laser output versus pump beam power (see Fig. 3). The measured laser emission versus pump wavelength is effectively broad and almost flat as expected from calculations. For better heat removal, a portion of the sample has been thinned by polishing the substrate down to a 100 μm thickness and glued to a copper heat sink. The pump beam is provided by a fiber coupled Coherent FAP system delivering up to 12 W cw in the pumping window

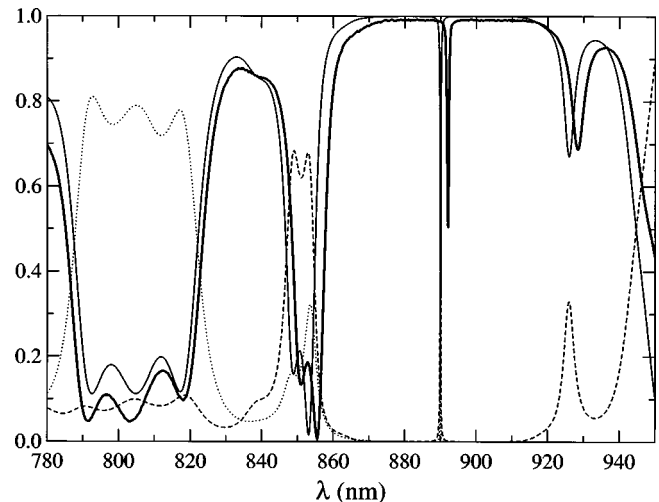


FIG. 2. Calculated reflectance (thin straight line), transmittance (dashed line), and absorption (dotted line) spectra for the optimized structure. The thick straight line is the measured spectra on the grown sample. The cavity resonance is around 890 nm and the pumping window ranges from 790 to 820 nm.

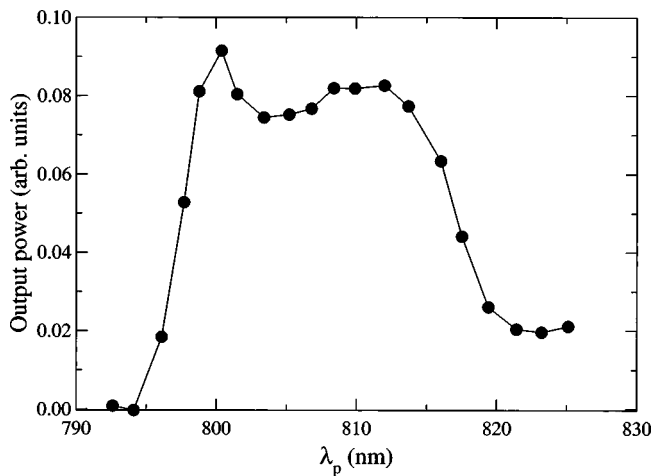


FIG. 3. Normal incidence pumping with Ti:sapphire laser on a small area of the sample above laser threshold at a pump wavelength λ_p . The measured output power is directly related to the absorption inside the cavity.

with a 1.5 nm linewidth. The beam is collimated and re-focused onto the sample thanks to a 2.5 mm focal length microscope objective (numerical aperture=0.9). The illuminated area has a top-hat shape profile and a diameter of 80 μm . Lasing is obtained at room temperature (Fig. 4) with long pump pulses (100 μs duration and 500 μs period) and a threshold of 11.5 kW/cm^2 , which corresponds to 580 mW of pump power incoming onto the sample. The output power delivered by the device is in the hundreds of microwatts

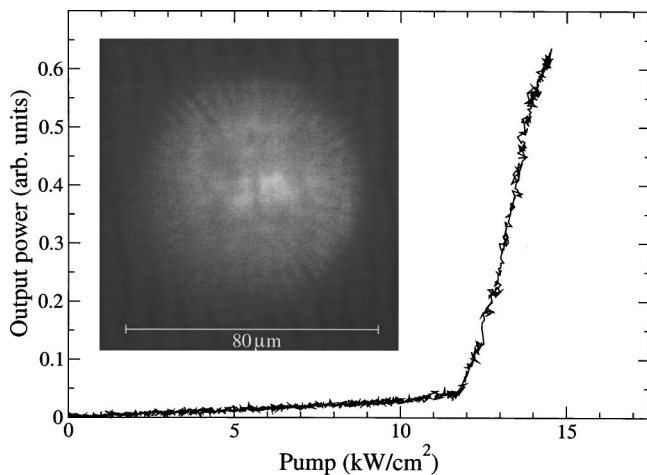


FIG. 4. Thinned sample output power vs input pump light power density for a top-hat shape pump profile of 80 μm in diameter. Inset: near-field image of the laser above threshold.

range for the maximum pump power used. The near-field image above threshold shows emission on the whole pumped surface. The emitted pattern is quite regular, as expected for a laser with a large number of lasing transverse modes, except at the border where radial stripes are visible. This pattern can be attributed to high-order flower-like Laguerre modes observed in broad-area VCSELs close to threshold.¹¹ It must be noted that with such large diameters, heat removal from the edges of the VCSEL is much less efficient than from the substrate.¹² Particular attention must then be paid to the soldering to the heat sink in order to evacuate the heat generated in the active medium itself. Indeed, the temperature dependence of the laser threshold shows that cw operation is expected at -3°C .

In conclusion, we have designed an optically pumped broad-area microcavity with enhanced absorption and threshold characteristics. The special multilayer mirrors design allows pumping with high-power fiber-coupled diode laser arrays and high numerical apertures. This is due to an optimization on both the absorption and the transmission around the pump wavelength. We show the quasi-cw laser operation obtained at room temperature on a bulk GaAs broad-area microcavity and a top-hat shape pump profile. This demonstrates the powerfulness and feasibility of this technique.

¹M. Grabherr, B. Weigl, G. Reiner, R. Michalzick, M. Miller, and K. Ebeling, *Electron. Lett.* **32**, 1723 (1996).

²M. Miller, M. Grabherr, R. King, R. Jäger, R. Michalzick, and K. Ebeling, *IEEE J. Sel. Top. Quantum Electron.* **7**, 210 (2001).

³S. Barland, J. Tredicce, M. Brambilla, L. A. Lugiato, S. Balle, M. Giudici, T. Maggipinto, L. Spinelli, G. Tissoni, T. Knödl, M. Miller, and R. Jäger, *Nature (London)* **419**, 699 (2002).

⁴V. Voignier, J. Houlihan, J. R. O. Callaghan, C. Sailliot, and G. Huyet, *Phys. Rev. A* **65**, 053807 (2002).

⁵K. J. Knopp, D. H. Christensen, and J. R. Hill, *Appl. Phys. Lett.* **69**, 3987 (1996).

⁶M. J. Bohn and J. G. McInerney, *Opt. Commun.* **117**, 111 (1995).

⁷M. Grabherr, S. Intemann, R. Jäger, R. King, R. Michalzick, H. Roscher, and D. Wiedenmann, *Proc. SPIE* **4994**, 83 (2003).

⁸Y. Ohiso, K. Tatenno, Y. A. Wakatsuki, H. Tsunetsugu, and T. Kurokawa, *IEEE Photonics Technol. Lett.* **8**, 1115 (1996).

⁹W. H. Press, S. A. Teukolsky, W. T. Vetterling, and B. P. Flannery, *Numerical Recipes in C: The Art of Scientific Computing*, 2nd Ed. (Cambridge University Press, Cambridge 2002).

¹⁰Y. Onishi, F. Koyama, and K. Iga, *Jpn. J. Appl. Phys., Part 1* **40**, 4920 (2001).

¹¹T. Ackemann, S. Barland, M. Cara, S. Balle, J. R. Tredicce, R. Jäger, M. Grabherr, M. Miller, and K. J. Ebeling, *J. Opt. B: Quantum Semiclassical Opt.* **2**, 406 (2000).

¹²Y. Ménesguen and R. Kuszelewicz, to appear in *IEEE J. Quantum Electron.* (2005).